

## Chapter 2

# The *DIRBE* Instrument

### 2.1 Design Goals

The *DIRBE* was designed to make an absolute measurement of the spectrum and angular distribution of the diffuse infrared background. The instrument covers the wavelength range from 1.25  $\mu\text{m}$  to 240  $\mu\text{m}$  in 10 bands with a design sensitivity per field of view on the sky of  $\lambda I_\lambda = 10^{-9} \text{ W m}^{-2} \text{ sr}^{-1}$  in each band after 1 year of observation. The instrument also measures two perpendicular components of linear polarization in its short wavelength bands at 1.25, 2.2, and 3.5  $\mu\text{m}$ . The polarization measurements were included to help distinguish the contribution to the infrared background from sunlight scattered by interplanetary dust and to help in modeling the spatial distribution of the interplanetary dust. Since the *DIRBE* optical axis is oriented  $30^\circ$  from the spin axis of the *COBE* spacecraft, it views half the sky every day at solar elongation angles ranging from  $\varepsilon = 64^\circ$  to  $124^\circ$  with many redundant scans. Over the course of six months, every celestial direction is redundantly sampled at all possible elongation angles in this range.

### 2.2 Instrument Description

The *DIRBE* is a cryogenically-cooled ten band absolute photometer that measures the difference between the sky brightness and a zero-flux internal surface using a tuning-fork chopper running at 32 Hz. The synchronously demodulated signal is averaged for  $\frac{1}{8}$ th of a second before transmission to the ground. A cold shutter can be closed to block the sky signal to measure instrumental offsets. *DIRBE* uses celestial objects and internal thermal reference sources for monitoring response stability, and celestial sources for absolute response calibration. The instrument design, together with the mission and spacecraft capabilities, were chosen to facilitate discrimination of emissions from the solar system and our Galaxy from that of an isotropic cosmic infrared background (CIB). Table 2.2-1 summarizes the instrument characteristics.

Table 2.2-1: Instrument characteristics

Telescope diameter (primary)	19 cm
Telescope type	Cryogenic off-axis folded Gregorian
Telescope effective focal length	14.24 cm
Instantaneous field of view (FOV)	$0^\circ 7 \times 0^\circ 7$
Instrument type	absolute photometer and polarimeter
Photometric bands ( $\mu\text{m}$ )	1.25, 2.2, 3.5, 4.9, 12, 25, 60, 100, 140, 240
Polarimetric bands ( $\mu\text{m}$ )	1.25, 2.2, 3.5

### 2.2.1 Optics and Baffling

The *DIRBE* optics were carefully designed for strong stray light rejection (Magner 1987). The configuration (Figure 2.2-1) includes re-imaging with both a secondary field stop and a Lyot stop, superpolished

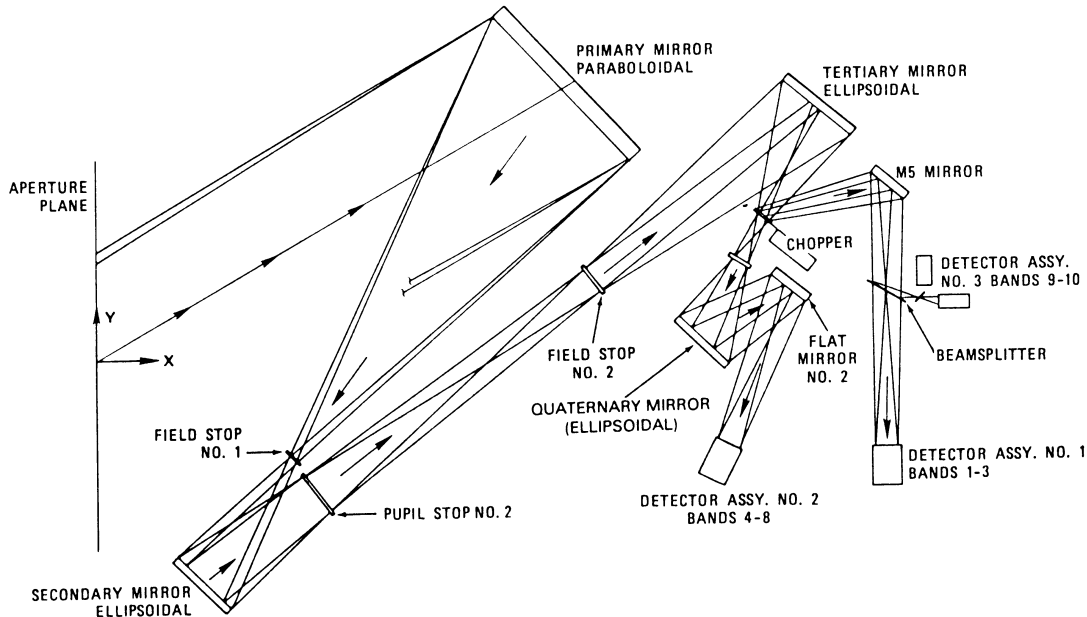


Figure 2.2-1: Optics diagram of *DIRBE*. The full beam shutter (not shown) was located at field stop 1. The cold beam stop (not shown), viewed by all detectors when not exposed to the sky (or shutter), was located to the left of the chopper blades in this Figure.

primary and secondary mirrors to further reduce scattered light, extensive internal baffling as well as a reflective forebaffle, and a complete light-tight enclosure within the *COBE* dewar to eliminate any optical cross-talk from the dewar or the other cryogenic instrument, *FIRAS*. Additional protection from the Earth and Sun are provided by the attitude control system and by the Sun-Earth shade surrounding the *COBE* dewar, which prevent any direct illumination of the dewar or instrument apertures from these omnipresent strong local sources.

The front end of *DIRBE* utilizes an off-axis folded Gregorian telescope with a 19 cm diameter off-axis segment of a parabolic mirror as the primary. There are no structural elements in the optical beam. Collimated incident light is imaged at the first field stop. An off-axis segment of an elliptical secondary forms an image of the primary at a pupil stop. This pupil stop (Lyot stop) is smaller than the image of the primary, blocking radiation diffracted from the primary mirror. The secondary mirror also images the first field stop at a second field stop. The second field stop is smaller than the first, blocking stray radiation scattered or diffracted at the first stop and setting the  $0.7 \times 0.7$  instantaneous field of view. An ellipsoidal tertiary mirror imaged the pupil (Lyot stop) at a tuning fork chopper with mirrored blades. In the chopper open position sky light reaches the elliptical quaternary mirror, which images the pupil via a folding flat onto detector assembly 2. With the chopper closed, the aspheric mirror (M5) reimages the pupil onto detector assemblies 1 and 3.

In this optical arrangement, all detector assemblies are located at a pupil image. Since the required sensitivity could be achieved with modest etendue in the first 8 bands ( $1-100 \mu\text{m}$ ), pupil division was employed to divide energy between bands, giving these bands an effective etendue of  $0.0044 \text{ cm}^2 \text{ sr}$ ; the 140 and  $240 \mu\text{m}$  bands used the entire entrance aperture and have an etendue of  $0.044 \text{ cm}^2 \text{ sr}$ .

All of the spectral bands view the same instantaneous  $0.7 \times 0.7$  field of view (FOV) simultaneously. Optical testing showed small misalignments of the beam centroids. Corrections for these small pointing

offsets are applied in the ground data processing (see §4.2.2 and Table 4.2-1). With this configuration, each detector assembly received radiation chopped alternately between the sky and the cold beam stop. The cold beam stop was a black enclosure maintained below 3° K, producing no detectable signal at any *DIRBE* wavelength. *DIRBE* sky measurements were thus continuously referenced to zero flux. Instrumental zero point offsets due to electronic pick-up or stray radiation could be measured by closing the full-beam cold shutter located at field stop 1 (see §4.5.2 for discussion of offset determination and correction).

### 2.2.2 Detector Assemblies

The detectors are arranged into three separate mechanical assemblies. Beamsplitters divide the light spectrally to direct the appropriate wavelengths to each detector assembly. The detector and filter characteristics and descriptions are shown in Table 2.2-2. Bands at 1.25, 2.2, and 3.5  $\mu\text{m}$  are each equipped with three detectors, one measuring total intensity and two additional detectors, each of which has a linear polarizer in front of it. Each detector channel in an assembly included a detector element, Winston cone condensing element, spectrally-defining filter, and a cold JFET and load resistor for preamplification.

Each detector element (except the bolometers) was mounted on a low heat capacity substrate which was weakly coupled thermally to the mechanical structure. The substrate included a heater element which was used to set an optimal DC operating temperature for that detector, and, where necessary, to provide thermal annealing of detector response changes due to passage through the South Atlantic Anomaly.

Table 2.2-2: Detector and filter characteristics

Band	$\lambda^a$ ( $\mu\text{m}$ )	$\Delta\nu_e^b$ (Hz)	Detector Type	Filter Construction <sup>c</sup>
1	1.25	$5.95 \times 10^{13}$	InSb <sup>d</sup>	Coated Glass
2	2.2	$2.24 \times 10^{13}$	InSb <sup>d</sup>	Coated Glass
3	3.5	$2.20 \times 10^{13}$	InSb <sup>d</sup>	Coated Germanium
4	4.9	$8.19 \times 10^{12}$	InSb <sup>d</sup>	MLIF/Germanium
5	12	$1.35 \times 10^{13}$	Si:Ga BIB	MLIF/Germanium/ZnSe
6	25	$4.13 \times 10^{12}$	Si:Ga BIB	MLIF/Silicon
7	60	$2.32 \times 10^{12}$	Ge:Ga	MLIF/Sapphire/KRS5/Crystal Quartz
8	100	$9.74 \times 10^{11}$	Ge:Ga	MLIF/KCl/CaF <sub>2</sub> /Sapphire
9	140	$6.05 \times 10^{11}$	Si/diamond bolometer	Sapphire/Mesh Grids/BaF <sub>2</sub> /KBr
10	240	$4.95 \times 10^{11}$	Si/diamond bolometer	Sapphire/Grids/BaF <sub>2</sub> /CsI/AgCl

<sup>a</sup> Nominal wavelength of *DIRBE* band.

<sup>b</sup> Effective bandwidth assuming source spectrum  $\nu I_\nu = \text{constant}$ .

<sup>c</sup> MLIF = multi-layer interference filter.

<sup>d</sup> Anti-reflection coated for the band center wavelength.

#### 2.2.2.1 Detectors

The *DIRBE* detectors are listed by band in Table 2.2-2. All of the detectors were custom-made. The InSb detectors for 1.25 – 4.9  $\mu\text{m}$  (bands 1 – 4) were 1 mm diameter photodiodes obtained from Cincinnati Electronics. The 12 and 25  $\mu\text{m}$  (band 5 and 6) Blocked Impurity Band (BIB) photoconductors each had a  $1 \times 1.75$  mm rectangular active area and were supplied by Rockwell. The Ge:Ga photoconductors used at 60 and 100  $\mu\text{m}$  (bands 7 and 8) had  $1 \times 1 \times 1$  mm dimensions and came from Infrared Labs.

The 140 and 240  $\mu\text{m}$  (band 9 and 10) detectors were fabricated at NASA/Goddard Space Flight Center (GSFC). The bolometers used Cr/Au resistive absorbing films on octagonal diamond substrates (2.75 mm across flats). The 140  $\mu\text{m}$  substrate was 18  $\mu\text{m}$  thick, while the 240  $\mu\text{m}$  substrate was 25  $\mu\text{m}$  thick. The absorbing film impedances were  $\sim 70\Omega$  per square, resulting in  $\sim 80\%$  absorption near band

center. The thermometers were boron-compensated Si cubes 0.25 mm on a side. Electrical contacts were made on two opposite faces using a degenerate As implant with a Cr/Au contact layer.

The detector response functions were measured at GSFC using a Nicolet Michelson Fourier Transform Interferometer Radiometer (FTIR) and a reference detector (a monolithic silicon bolometer). The optimal detector temperatures and bias voltages found in the laboratory were similar to those determined to give the best performance on orbit (see Table 3.2-1).

#### 2.2.2.2 Filters

The *DIRBE* filters are listed by band in Table 2.2-2. Filters for the 1.25 – 4.9  $\mu\text{m}$  bands consisted of multi-layer interference coatings on transparent substrates and were supplied by the AGA Corporation of Sweden (presently Spectrogon, AB). The 12 – 100  $\mu\text{m}$  filters consisted of multi-layer interference coatings stacked atop infrared-active crystals anti-reflection coated with polyethylene (Infrared Labs). The 140 and 240  $\mu\text{m}$  filters were stacked infrared-active crystals with inductive mesh grids (Perkin-Elmer). All of the filters were paralene encapsulated and anti-reflection coated. The filter transmission and beamsplitter characteristics were measured at  $< 10$  K using the Nicolet FTIR at GSFC (Heaney *et al.* 1986).

Not counting the polarizers, there were two beamsplitters. One beamsplitter, consisting of a Cr/Au inductive mesh on a sapphire substrate, reflected long wavelengths and transmitted short wavelengths, and was used to separate the 1.1 – 4.0  $\mu\text{m}$  bands (detector assembly 1; see Figure 2.2-1) from the 120 – 300  $\mu\text{m}$  bands (assembly 3). The second beamsplitter, a mesh filter on a Si substrate, was used to separate the 140 and 240  $\mu\text{m}$  bands.

#### 2.2.2.3 Spectral Response Functions

The *DIRBE* passbands were formed by the convolution of filters, detector response functions, and dichroic beamsplitters. The filter and detector response functions from 1.25 – 100  $\mu\text{m}$  (bands 1 – 8) and the system response functions at 140 and 240  $\mu\text{m}$  (bands 9 and 10) were measured at GSFC. Out-of-band leaks were measured to 1 part in at least  $10^4$  (in some bands to a part in  $10^8$ ) and determined to satisfy the (to-be-provided) requirements.

Though the attempt was made to produce the same spectral response as *IRAS* in the 12 – 100  $\mu\text{m}$  bands, there were several significant differences. The long-wavelength cutoff of the BIB detector used in the *DIRBE* band 6 was  $\sim 27\mu\text{m}$ , as opposed to 30  $\mu\text{m}$  for the Si:Sb photoconductor used in *IRAS* band 2. The *DIRBE* 60  $\mu\text{m}$  response was measured and found to have a long-wavelength cutoff at 70  $\mu\text{m}$  rather than at 78  $\mu\text{m}$  as in the *IRAS* case (see the *IRAS Catalogs and Atlases Explanatory Supplement*, p. II-18).

Normalized system spectral response functions are shown in Figure 2.2-2, tabulated in Appendix A, and delivered as a data product in ASCII form (see §5.9.2).

#### 2.2.2.4 Polarizers

In addition to the full intensity channels (designated ‘A’) in the 1.25, 2.2 and 3.5  $\mu\text{m}$  bands, two detectors were used to make polarization measurements in each of these bands. Channels designated ‘B’ and ‘C’ contain polarizers whose transmission axes are orthogonal and fixed inside the *DIRBE* as well as band-defining spectral filters and detectors like those used in the corresponding A channels. The C channels have axes of maximum transmission aligned along the component of the *DIRBE* scan direction attributable to the spacecraft spin. The polarizing elements are 5000 line/mm aluminum grids etched on sapphire substrates.

### 2.2.3 Thermal Control

Temperatures inside the cryostat (see §2.3.7) were maintained stable and below 1.6 K while the cryogen supply lasted except during occasional transient events (see §3.4.3). The external surfaces of the dewar and surrounding system were designed to minimize the dewar main shell temperature and, therefore, heat loads to the cryogen. A Sun–Earth shield (§2.3.8) protected the *DIRBE* and dewar apertures

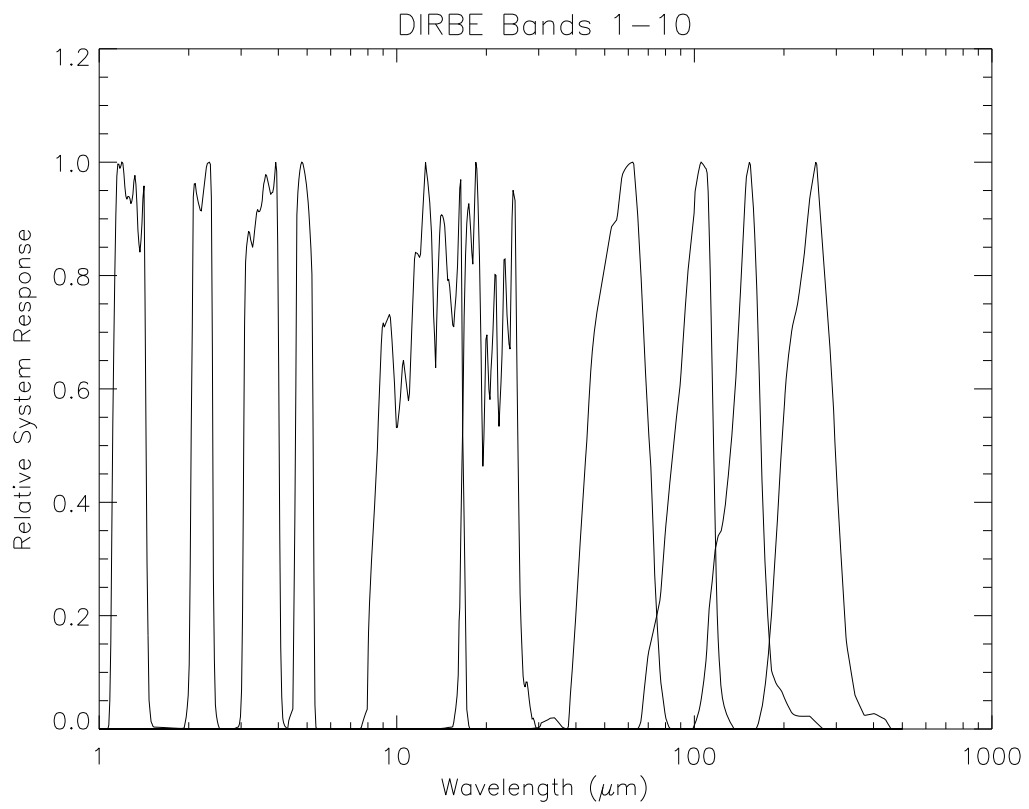


Figure 2.2-2: Normalized system spectral response

from direct solar radiation when the *DIRBE* line of sight was pointed more than  $60^\circ$  from the Sun, a constraint which was maintained throughout the mission.

## 2.2.4 Calibration

### 2.2.4.1 Cold Chopper

Absolute surface brightnesses are measured by chopping between the sky signal and the cold internal beam stop, which is a stable, zero-flux reference at the wavelengths of the *DIRBE*. The cryogenic tuning fork chopper operates at 32 Hz and is located at a pupil image (see Figure 2.2-1).

### 2.2.4.2 Shutter

Instrumental offsets were determined by closing off the sky from the instrument with a cold shutter located at the prime focus (Field Stop No. 1 in Figure 2.2-1; the shutter is not shown in the figure). The shutter was demonstrated to attenuate saturation-level sky signals to well below instrument noise levels at all *DIRBE* wavelengths. The shutter closed condition with the internal reference source (see §2.2.4.3) turned off defined the zero sky brightness signal for *DIRBE* measurements.

### 2.2.4.3 Internal Reference Sources

The back of the shutter has a mirror which allows light from an internal reference source (IRS) system located out of the path of the sky beam to reach the detectors via the secondary and subsequent mirrors only when the shutter is closed. Measuring the instrument signal with the shutter closed and the IRS off permits determination of instrumental noise levels and electrical and radiative offsets. Turning on the IRS at fixed levels permits monitoring of system gain stability. Calibration procedures are described in §3.3.

The IRS system consisted of four thermal sources, only one of which was designated the primary source at any given time. When the source initially used as the primary failed, the source originally designated “secondary” was substituted (see §3.5.2).

## 2.2.5 Electronics

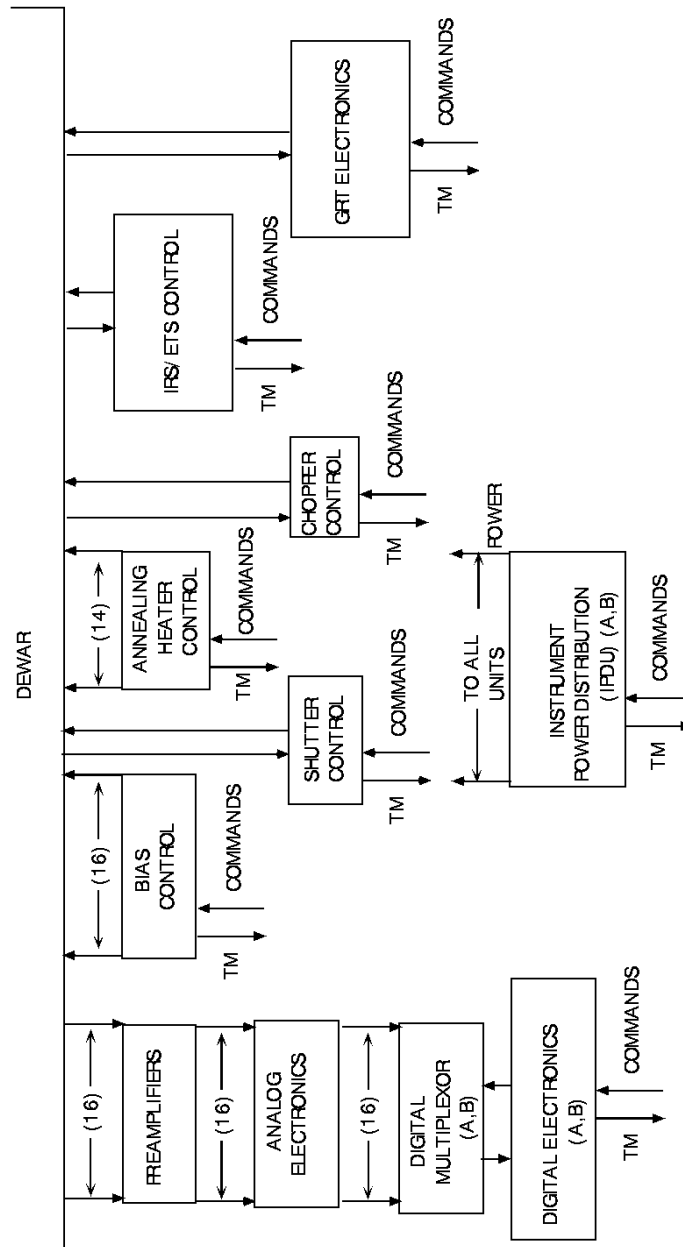
The *DIRBE* instrument electronics consist of the individual detector’s analog electronics and the common electronics for collecting, digitizing, and processing the data (Figure 2.2-3). With the exception of the detector-unique analog electronics, all of the electronic elements were redundant. These units consisted of two duplicate (referred to as unit A or B) instrument power distribution units (IPDU) and two digital electronics units (DEU). Any pair consisting of an IPDU and a DEU was valid and the subsystem was tested on the ground in all possible configurations. Full system performance was tested only using all A units, then all B units. In flight the B units were used; there was never a need to switch to a redundant *DIRBE* electronics unit.

The IPDU conditioned power from the *COBE* solar arrays and from the battery, which was only used during short “eclipse” periods near the June solstices (see §2.3.3). The IPDU electronics also monitored analog and digital electronics and configuration functions, and it provided a command interface for control and monitoring of power functions. All power monitoring signals were inserted into the telemetry stream on a sampled basis, and no signal was sampled less frequently than once per 32 seconds.

Each DEU contained a TI9900 microprocessor which digitized the analog signals from each of the detectors using an analog multiplexer and a 12-bit successive approximation analog-to-digital converter. Advantage was taken of the microprocessor’s inherent flexibility to enable operation of the instrument in a number of modes (see §2.2.6).

A cryogenic JFET source follower on each detector reduced the output impedance. Remaining elements of the transimpedance preamplifiers for the photovoltaic and photoconductive detectors were located outside the dewar; high gain preamplifiers were used for the bolometric detectors.

The electronic gain of each individual detector channel was commandable over a factor of 30. This capability was included to protect against uncertainty in the sky brightness, to allow for possible optical



**DRBE ELECTRONICS BLOCK DIAGRAM**

Figure 2.2-3: Electronics block diagram of *DIRBE*

efficiency degradation, and to permit gain readjustment in some bands after cryogen exhaustion. To achieve the required dynamic range at each commandable gain, each detector output was sampled at 256 Hz at the nominal commanded gain (low) and at 16 times that gain (high). The on-board micro-processor was programmed to choose the highest non-saturated gain for signal processing calculations and insertion into the telemetry. An output bit indicated which gain (high or low) was chosen for each detector's output. Nominal commanded gains were set so that non-saturated signals were produced in the high gain state over most of the sky.

The stability and precise gain ratios of the analog electronics could be determined by injecting an electronic test signal (ETS) into the analog chain in place of the preamplifier output. This test signal was generated in the same unit that provided the drive signals for the IRS.

The shutter and the IRS were controlled by the DEU. For internal calibration and stability monitoring, several programmed sequences of IRS levels were used during flight. The sequences were arranged to assure that each detector was stimulated at several levels in its dynamic range. Programmed sequences were tailored to each of the four IRS sources to produce similar output levels. This was required to account for differences in optical outputs of the sources. Celestial sources provided a long-term monitor of IRS stability and detector performance (see Chapter 4). The IRS and its drive electronics were designed to be highly stable over time scales of at least days.

## 2.2.6 DIRBE Operating Modes

As noted in §2.2.5, the *DIRBE* instrument could be operated in a variety of modes. Most of these modes were used for instrument diagnostics both on the ground and in orbit. Because the mission proceeded nominally, about 95% of the time in orbit was spent in the primary science data-gathering mode (SDM) or in the mode used for calibration and stability monitoring (CAL). In CAL mode, the instrument shutter is closed for internal calibration and offset monitoring; the SDM and CAL modes are otherwise the same.

In SDM, to enhance the signal-to-noise ratio and reduce the bandwidth required to send data for each detector to the ground, data from four chopper cycles were combined on-board. At the chopper oscillation frequency, 32 Hz, four cycles lasted  $\frac{1}{8}$ th of a second, during which time 32 samples were collected. The output signal from the  $i$ th detector,  $S_i$ , was digitally demodulated synchronously with respect to the phase of the chopper and was, specifically,

$$S_i = \sum_{s=1}^{32} D_{i,s} M_{i,s}, \quad (2.1)$$

where  $D_{i,s}$  represents detector sample  $s$  and  $M_{i,s}$  is a mask containing only values of  $\pm 1$ . The phase of the mask was adjusted so that  $M$  would turn out to be  $+1$  for samples obtained when the detector was exposed to the sky signal and to  $-1$  when the chopper was seen. In practice, a phase setting was sought that would maximize the output signal subject to the condition that the mask be symmetrically positioned with respect to the chopper cycles in order to reject to first order the bias inherent in digitizing a smoothly varying sky signal.  $S_i$  represents the average response of the detector to the sky over  $\frac{1}{8}$ th of a second, and these  $\frac{1}{8}$ -second demodulated samples were recorded on the spacecraft tape recorder for telemetry to the ground. To ensure that the wide dynamic range required by some bands could be achieved, data compression to 12 bits was performed on-board and the result was reconstructed on the ground to 0.25% precision or better. Section 4.2.2 describes how the detector sampling time was set to achieve beam alignment.

Complementary to SDM, there were three special data sampling modes in which synchronous demodulation was *not* performed. In snapshot mode (SNAP), either all 8 samples per chopper cycle were telemetered for two selectable detectors, or 16 samples were delivered for one detector. In continuous burst mode (CBM), 4 samples per chopper cycle for two selectable detectors were included in the telemetry. In single channel mode (SNG), data from a single selected detector were telemetered continuously at 4 samples per chopper cycle.

There were two calibration modes in addition to CAL mode. In electronic test signal mode (ETS), the analog electronics were stimulated by the built-in test signal generator. During annealing periods,



special settings of detector heaters and IRS sources were used to remove the effects of nuclear particle bombardment from the detectors (see §§3.4.1 and 3.5.1). In annealing mode (ANL), the normal detector data were replaced by data on the setting of the detector heaters and the DC output from the detectors (see §2.2.2).

A stand-by mode (STM) was included for safety. In this mode, the firmware used by the on-board microprocessor could be dumped into the telemetry stream in place of instrument data.

## 2.3 The Instrument in Context: the COBE Satellite

Boggess *et al.* (1992) described the design of the Cosmic Background Explorer (*COBE*) and its performance two years after launch. This section and section 3.1.1 include *DIRBE*-related parts of the Boggess *et al.* paper. The *COBE* mission design is described here, and spacecraft performance in flight is summarized in Table 3.1-1. The *DIRBE* performance in flight is discussed in Chapters 3 and 4.

### 2.3.1 Mission Concept

To achieve the full benefit of space observations, a goal of the *COBE* mission and instrument design was that measurements would be limited ultimately by our ability to identify and model the various components of the astrophysical foreground sources in order to discriminate between them and the cosmic background emission. This goal drove the design of the mission strategy, the spacecraft and operations, and the choice of instruments. Basic elements in the mission strategy were the requirements for highly redundant full sky coverage and for sufficient time in orbit to achieve necessary sensitivity and evaluate potential sources of systematic errors in the observations. Other elements in the strategy were the needs for on-board instrument calibration and time for frequent checks of calibration stability. To reduce known sources of systematic errors, the mission orbit, spacecraft attitude and instrument enclosures were designed to eliminate direct exposure to Sun and Earth radiation and to maintain a well-controlled thermal environment for the instruments. Instrument and spacecraft design included efforts to minimize radio frequency contamination and interference from sources of stray radiation. Finally, the instruments were chosen to measure specific attributes of the cosmological backgrounds and also, through their complementary spectral coverage, to enable the modeling and subtraction of foreground emissions. Early descriptions of the mission concept were given by Mather (1982) and by Gulkis, Lubin, Meyer, & Silverberg (1990).

The three scientific instruments are the Far Infrared Absolute Spectrophotometer (*FIRAS*), the Differential Microwave Radiometers (*DMR*), and the Diffuse Infrared Background Experiment (*DIRBE*). The *FIRAS* objective is to make a precision measurement of the spectrum of the cosmic microwave background (CMB) from 1 cm to 100  $\mu\text{m}$ . The *DMR* objective is to search for CMB anisotropies on angular scales larger than  $7^\circ$  at frequencies of 31.5, 53, and 90 GHz. The *DIRBE* objective is to search for a CIB by making absolute brightness measurements of the diffuse infrared radiation in 10 photometric bands from 1.25  $\mu\text{m}$  to 240  $\mu\text{m}$  and polarimetric measurements from 1.25  $\mu\text{m}$  to 3.5  $\mu\text{m}$ .

The need to control and measure potential sources of systematic errors required an integrated design and operations concept. It led to the requirements for an all-sky survey and a minimum time in orbit of six months, and imposed constraints on the permitted amount of radiative interference from local sources such as the Earth, Sun, Moon, and radio interference from the ground, *COBE* spacecraft and other satellites. The instruments required temperature stability to maintain gain and offset stability, and a high level of cleanliness to reduce the entry of stray light and thermal emission from particulates. The control of systematic errors in the measurement of the CMB anisotropy and the need for measuring the zodiacal cloud at different solar elongation angles for subsequent modeling required that the satellite rotate. The choice of orbit, within the constraint of available launch vehicles, was also an important consideration in minimizing systematic errors.

The major components of the satellite were the instrument module and the spacecraft module. The instrument module contained the scientific instruments and some of their electronics, a superfluid He dewar, and a Sun-Earth shield. The spacecraft module included most instrument electronics, spacecraft subsystems including the attitude control system, command and data handling system, power system,

solar panels, two omnidirectional antennas, and necessary support structures. These components are shown schematically in Figure 2.3-1.

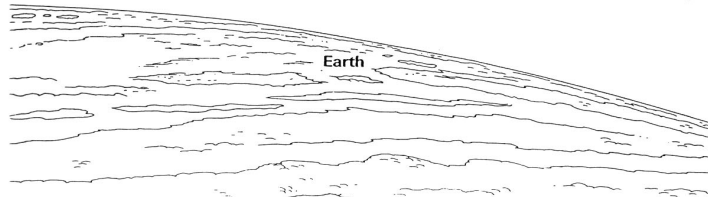
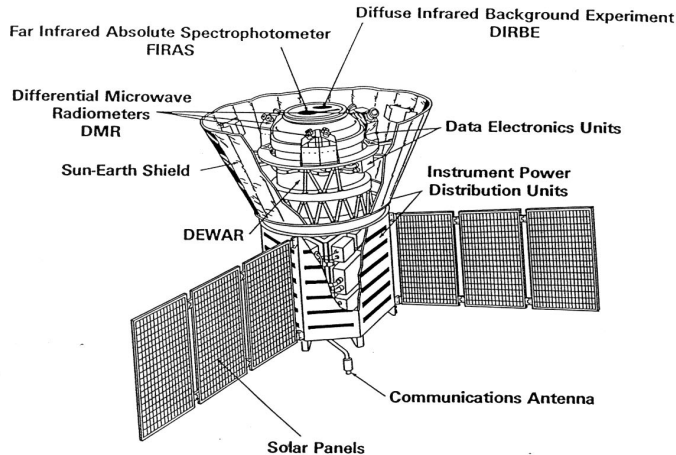


Figure 2.3-1: Artist cutaway drawing of the major components on *COBE*, showing the locations of the three scientific instruments.

### 2.3.2 The Orbit

The overriding considerations in choosing the orbit were the need for full sky coverage, the need to eliminate stray radiation from the instruments, and the need to maintain thermal stability of the dewar and the instruments. In near-Earth orbit, the Sun and Earth are the primary sources of thermal emission and it is necessary to ensure that neither the instruments nor the dewar are exposed to their radiation. A circular Sun-synchronous orbit can satisfy these requirements throughout the year. In a Sun-synchronous orbit, the inclination and altitude are chosen so that the orbital plane precesses  $360^\circ$  in one year due to the Earth's gravitational quadrupole moment. For *COBE*, a 900 km altitude orbit was chosen, requiring a  $99^\circ$  inclination. A 900 km altitude was within the launch capabilities of the Shuttle (with an auxiliary propulsion system on *COBE*) or a Delta rocket. This altitude is a good compromise between contamination from the Earth's residual atmosphere, which increases at lower altitude, and interference due to charged particles in the Earth's radiation belts at higher altitudes. A 6 PM ascending node was chosen for the *COBE* orbital plane; this node follows the terminator (the boundary between sunlight and darkness on the Earth) throughout the year. By continuously reorienting the spacecraft spin axis to about  $94^\circ$  from the Sun and close to the local zenith, the Sun and Earth were kept below the plane of the shield. In this observing mode, the spacecraft central axis scanned the full sky every six months. The orbit is shown schematically in Figure 2.3-2. The orbital period is 103 minutes, giving almost exactly 14 orbits per day.

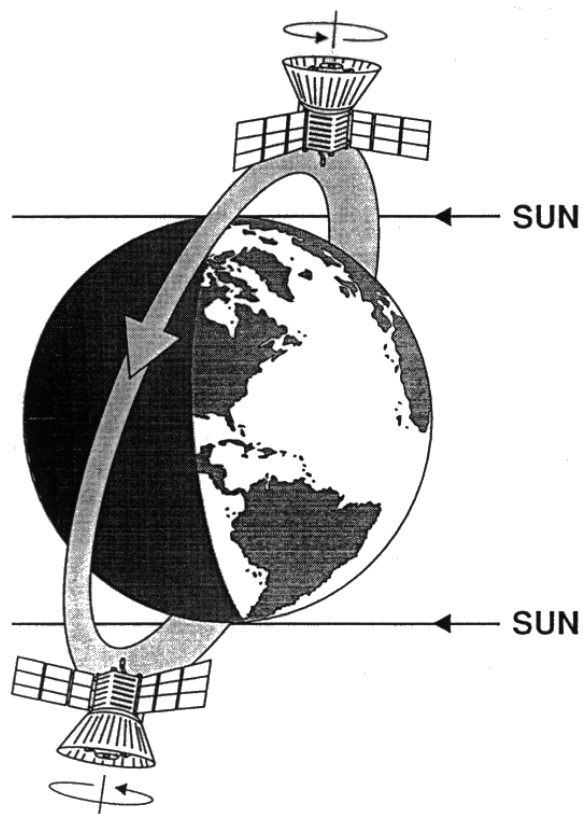


Figure 2.3-2: Schematic drawing of *COBE* in orbit. *COBE* is shown in a high-inclination orbit with its axis of rotation always pointing away from the Earth and about  $90^\circ$  from the Sun.

### 2.3.3 Attitude Control

It was necessary to spin the spacecraft to attain the scientific objectives of measuring the CMB anisotropy and searching for a CIB. As will be discussed in more detail below (and illustrated in Figure 2.3-3), the *FIRAS* optical axis pointed along the spin axis while the *DIRBE* and *DMR* beams

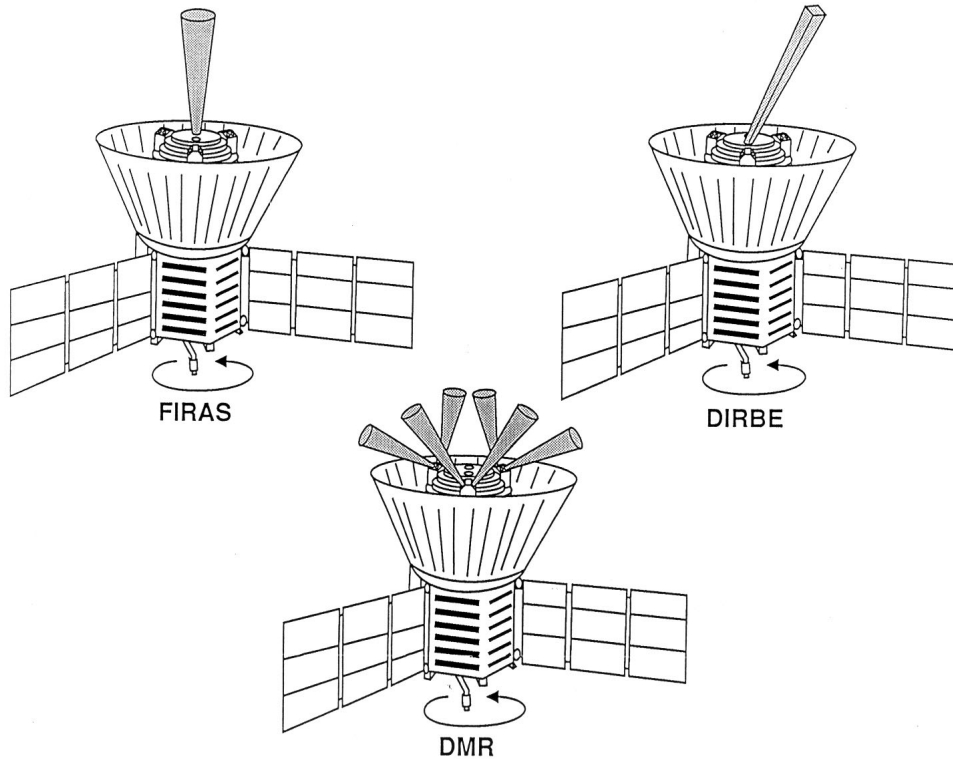


Figure 2.3-3: Schematic drawing of the viewing direction for each of the three *COBE* instruments with respect to the spin axis of the spacecraft.

pointed  $30^\circ$  from the axis. The spin allowed *DIRBE* to measure the emission and scattering by the zodiacal dust cloud over a range of solar elongation angles for each celestial direction, which aids in the discrimination and subsequent modeling of zodiacal radiation. The 0.8 rpm spin rate was chosen to be fast enough to reduce the noise and systematic errors that could otherwise arise from radiometer gain and offset instabilities. The spin axis was tilted back from the orbital velocity vector as a precaution against possible deposition of residual atmospheric gas on the cold optics and against a possible infrared glow that would arise from fast neutral particles hitting surfaces at supersonic speeds. (The tilt-back varied a few degrees about  $96^\circ$  during each orbit.) The axis of the spacecraft was also tipped to angles between  $92^\circ$  and  $94^\circ$  from the Sun to reduce the amount of sunlight reflected or scattered from the edge of the shield into the instrument apertures and dewar.

A sophisticated attitude control system met the unique requirements of slow rotation and 3-axis control. This was implemented by using a pair of inertia wheels (yaw angular momentum wheels), with their axes oriented along the spacecraft spin axis. These wheels carried an angular momentum opposite that of the entire spacecraft to create a zero net angular momentum system. The spacecraft orientation was controlled by three reaction wheels with spin axes  $120^\circ$  apart in the plane perpendicular to the spacecraft spin axis and by electromagnetic coils (torquer bars) that interact with the Earth's magnetic field.

The attitude of the spacecraft was measured and maintained by a redundant set of sensors and servo

systems. Earth and Sun sensors (one of each on each of the three transverse control axes) provided control signals to point the spin axis away from the Earth and at least  $90^\circ$  from the Sun. Rate damping and fine resolution attitude sensing were provided by six gyros, one on each transverse control axis and three on the spin axis. The system was redundant in that stable operation was achievable with one or perhaps two of the transverse control axes disabled, and with only one spin axis gyro operable.

Coarse attitude parameters were calculated by using telemetered data from the attitude control sensors. The Sun and Earth directions were measured in spacecraft body coordinates and transformed to inertial coordinates using the spacecraft ephemeris. These were then used to compute quaternions and rotation matrices describing the spacecraft orientation. The data were smoothed and interpolated using the gyro signals to produce attitude solutions good to  $4'$  ( $1\sigma$ ), adequate to meet the initial requirements for the *FIRAS* and *DMR*. The *DIRBE*, with its smaller beam size ( $0.7^\circ$  rather than  $7^\circ$ ), required a more accurate attitude solution. This fine aspect was determined by using gyro data to interpolate between the positions of known stars detected in the *DIRBE* short wavelength bands. The fine aspect solution was accurate to  $1.5'$  ( $1\sigma$ ) and was used in the analysis of data from all three instruments.

There was an unavoidable radiative perturbation to the instruments from the Earth in the chosen orbit and spacecraft attitude. At 900 km altitude, the Earth's limb is  $118^\circ$  from the zenith. Since the attitude control system maintained the axis of the satellite pointing away from the Earth and  $94^\circ$  from the Sun, the Earth limb did not rise above the plane of the Sun–Earth shield for most of the year. However, since the Earth's axis is tilted  $23.5^\circ$  from the ecliptic pole, the angle between *COBE*'s orbital angular momentum vector and the ecliptic plane varied through the seasons from  $-14.5^\circ$  to  $+32.5^\circ$ . As a consequence, the combination of the tilt of the Earth's axis, the orbit inclination, and the offset of the spacecraft spin axis from the Sun brought the Earth limb above the shield for up to 20 minutes per orbit near the June solstices. During this period the limb of the Earth rose a few degrees above the plane of the shield for part of each orbit, while on the opposite side of the orbit the spacecraft went into the Earth's shadow. To minimize risk, this “eclipse season” was placed as far as possible after launch by locating the ascending node of the orbit over the evening terminator; thus, eclipses occurred near the south pole around the summer solstices.

### 2.3.4 Sky Scan Strategy

The scan strategy was governed by the requirement for all-sky coverage and the need for many scans of each pixel on the sky. Many scans build up the signal-to-noise ratio and allow tests for systematic errors by multiple measurements of the same part of the sky under different environmental conditions, instrument parameters, and observing times.

Each scientific instrument had a unique scan pattern that depended upon its orientation on the satellite (Figure 2.3-3). The *DIRBE*, located inside the dewar, viewed  $30^\circ$  from the spin axis to provide data over solar elongation angles ranging from about  $64^\circ$  to  $124^\circ$  during each spacecraft rotation. Combined with the continuous pitching of the spacecraft to maintain an anti-Earth orientation, the spinning motion caused *DIRBE* to trace out a helical pattern on the sky and to sample half of the sky every day. Figure 2.3-4 shows the coverage achieved in a typical orbit.

Precession of the orbit caused the pattern to move about one degree per day, resulting in complete sky coverage within four months and more uniform sampling in six months. A comparison of the coverage achieved after various time intervals is given in Figure 2.3-5.

### 2.3.5 Power

Three solar array wings, deployed after launch, provided power for the spacecraft and instrument electronics. Each wing consisted of three panels with solar cells on both sides. The arrays were designed for a minimum lifetime of one year to maintain a peak capacity of approximately 1280 W at launch and an average capacity of 750 W at the end of the first year. The actual performance at the end of the first year had diminished by about 3%. The nominal spacecraft and instrument power load was 542 W.

Power generated in the solar arrays was supplied directly to the spacecraft and instrument subsystems through a regulated +28 V bus. The power system operated at close to 100% efficiency by taking

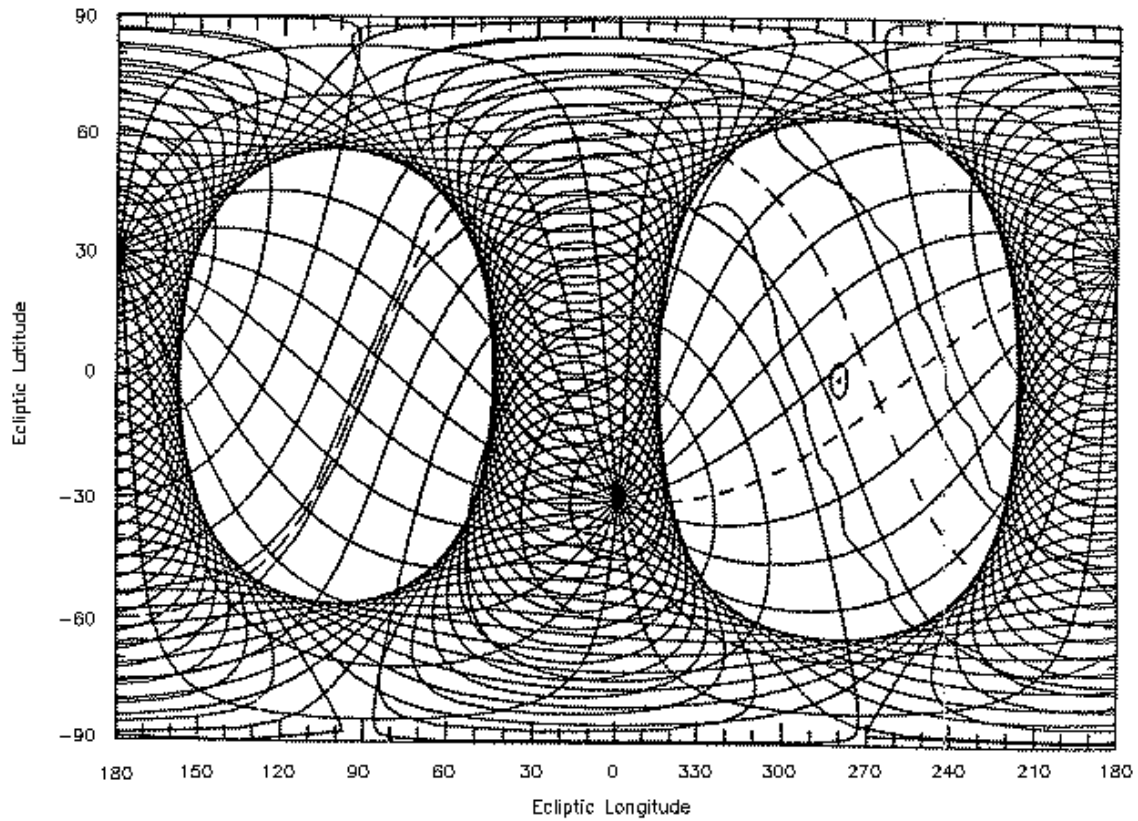


Figure 2.3-4: The track of the *DIRBE* line of sight on the sky over the course of one orbit on 1990 January 1. The sky is presented in ecliptic coordinates, with an overlay grid of Galactic coordinates. The contour lines surrounding the Galactic equator (long dashes) outline the rough appearance of the Milky Way.

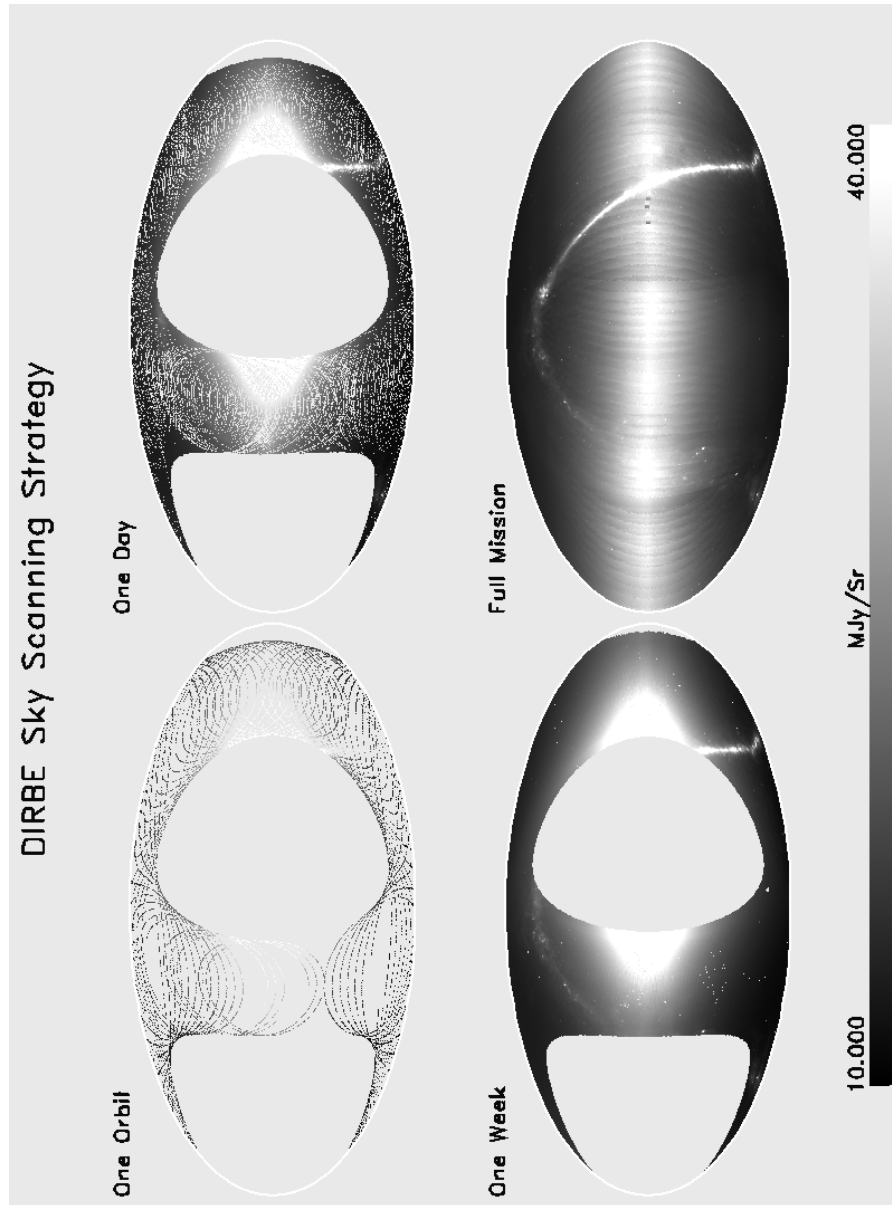


Figure 2.3-5: *DIRBE* sky coverage achieved for a typical orbit, a day, a week, and for the entire cryogenic mission. The maps shown depict  $12 \mu\text{m}$  emission in an Ecliptic Mollweide projection.

advantage of the nearly constant solar illumination provided by the orbit and spacecraft spin. Bus voltages were maintained by shunt regulators which radiated excess power into space. The 20 minute power transients during the eclipse season were smoothed by batteries.

A significant effort was made in developing spaceworthy low noise and RF-free power supplies and power distribution systems for the instruments. The low-noise sections had their own DC-DC power converters with separate grounds, multiple shields, and nested sub-regulators.

### 2.3.6 Communication

*COBE* required a special design for satellite commanding, tracking, and data retrieval. It had two antennas, one to communicate with the Tracking and Data Relay Satellite System (TDRSS), and the other to transmit data stored on tape recorders directly to the ground. The antennas, which were deployed after launch, were located on a mast at the bottom of the spacecraft.

The TDRSS link transmitted commands for tracking, spacecraft attitude maneuvers, and control of the instruments. It was also used to establish a short (10-20 minutes) real-time data flow, approximately every other orbit, from the satellite to the operations control center at the NASA Goddard Space Flight Center (GSFC) via the ground station at White Sands, NM.

The primary data flow was stored on one of two onboard tape recorders and read out daily directly to the NASA receiving station at the Wallops Flight Facility. The *COBE* near-polar orbit provided a minimum of two morning and two evening opportunities for transmission of the stored data. Both the stored and real-time data were relayed to the Payload Operations Control Center at GSFC for satellite health and safety monitoring and engineering trend analysis. The data were also relayed to the analysis center for quick-look processing. An edited tape of the tape recorder dump was received 24-48 hours after contact, and these data were used for final science data processing.

The spacecraft electronics included a command and data handling system that stored and decoded the commands received from the ground, collected data from the instruments and spacecraft at the rate of 4 kbps, and prepared data for transmission to the ground. The onboard tape recorders and data system allowed 24 hours of data to be transmitted to the ground in 9 minutes. Each instrument had a separate data stream located within a fixed part of the telemetry format. The data rate allocations for *DIRBE*, *FIRAS*, and *DMR* are 1716, 1362 and 250 bps, respectively. The remainder of the telemetry was assigned to spacecraft subsystems.

### 2.3.7 The Dewar

The dewar was a 650 liter superfluid helium cryostat designed to keep the *FIRAS* and *DIRBE* instruments cooled to less than 1.8 K for a minimum of six months. The *COBE* dewar was similar to that flown on the *IRAS* mission (Neugebauer *et al.* 1984). An aperture cover, sealing the dewar, permitted calibration and performance testing of the cryogenic instruments prior to launch. A contamination shield attached to the inside of the dewar cover protected the *DIRBE* primary mirror from particulate or gaseous contamination. It also protected *DIRBE* from emission from warm parts of the cryostat during ground testing. In orbit, the helium effluent was vented along the spin axis near the communications antennas.

### 2.3.8 The Sun-Earth Shield

The conical Sun-Earth shield protected the scientific instruments from direct solar and terrestrial radiation and provided thermal isolation for the dewar. The shield also provided the instruments with isolation from Earth-based RFI and from the spacecraft transmitting antenna. The shield was made of 12 honeycomb panels covered with multilayer insulating (MLI) blankets, alternating with flexible MLI segments. The outer layer of the MLI was aluminized Kapton to resist degradation due to the orbital bombardment by monatomic oxygen. The upper portion of the inner surface of the shield was covered with low emissivity aluminum foil to provide a high quality surface viewing the instrumentation. The shield was designed to be flexible and folded to fit within the Delta rocket fairing for launch.